Quantitative experimental study of the free decay of quasi-two-dimensional turbulence

O. Cardoso, D. Marteau, and P. Tabeling
Laboratoire de Physique Statistique, Ecole Normale Supérieure, 24, rue Lhomond, 75231, Paris, France
(Received 2 August 1993)

A quantitative experimental study of freely decaying quasi-two-dimensional turbulence is presented. The flow is produced in a thin layer of electrolyte by using a steady, spatially periodic, electromagnetic forcing. The particle-image-velocimetry method is used to determine the instantaneous velocity field, the vorticity field, and the stream function. Global quantities, such as the energy, the enstrophy, and the kurtosis of the vorticity distribution are measured, and geometrical properties, such as the number of eddies, their size, and their mean separation, are determined. Unexpected characteristics are obtained, revealing the existence of a new form of quasi-two-dimensional turbulence, which we call *liquid*.

PACS number(s): 47.27.−i

I. INTRODUCTION

Understanding and modeling two-dimensional turbulence are important issues of fluid mechanics and have many implications in geophysics and astrophysics. Much progress has been done on the problem these past years, partly because of the considerable amount of information originating from numerical simulations of the Navier-Stokes equations. Various aspects of two-dimensional turbulence have thus been investigated with new ideas such as the decay, the forced regime, or the statistical equilibrium. The importance of coherent structures, and the dynamical role of vortex filamentation among other phenomena, have been widely discussed [1–4].

The problem that we address here, from the experimental point of view, is the free decay of turbulence in extended systems, i.e., including initially a large population of vortices. The phenomenology of the decay process in such systems is now well established, at least in its main aspects: one finds, both numerically and experimentally, that large-scale structures are generated by successive merging of like-sign vortices. There are also many other phenomena, such as vortex stripping [5], dipole propagation, recombination of vortex filaments, etc., which form the intricate world of vortex dynamics, and one would, in principle, need a considerable amount of information to describe completely the decay process; the question of the relevance of a statistical approach arises and has still not received a definite answer. This approach has been proposed first by Batchelor, in a pioneering paper [6], which consists several important results about two-dimensional turbulent flows. In this approach, the statistics of the decay regime, characterized by geometrical and dynamical indicators, is determined. The argument used by Batchelor in this study is dimensional: It is based on the assumption that, during the decay phase, all the quantities related to the flow depend only on the total kinetic energy E (which is an invariant) and the time t. The corresponding laws then read:

$$r(t)\sim a(t)\sim\sqrt{E}\,t,\quad \rho(t)\sim\frac{1}{Et^2},\quad Z(t)\sim\frac{1}{t^2},\quad\text{and}\quad \omega_{\text{ext}}(t)\sim\frac{1}{t}\ , \tag{1}$$

where $a(t)$ is the mean size of vortices, $r(t)$ their mean separation distance, $\rho(t)$ the density of vortices, $Z(t)$ the enstrophy, and ω_{ext} the vorticity extremum of the system. Such laws infer, among other consequences, that the mean size of the vortices increases with time, which is in qualitative agreement with the observations.

Actually, these laws are not observed in the numerical simulations of freely decaying turbulence. One of them, due to McWilliams [4], clearly shows that (1) does not describe quantitatively the decay process. Some time after, Carnevale *et al.* [7] proposed a new statistical theory, which is also based on dimensional arguments, and which assumed the existence of another conserved quantity—the extremum vorticity ω_{ext}—during the decay phase. Such an assumption is justified, to some extent, by the Helmholtz theorem, and is found consistent with the numerical simulations mentioned above [4]. Using the total kinetic energy E and the maximum vorticity ω_{ext}, one can form a length scale λ and a time scale τ, according to the relations

$$\tau=\frac{1}{\omega_{\text{ext}}}\quad\text{and}\quad\lambda=\frac{\sqrt{E}}{\omega_{\text{ext}}}\ . \tag{2}$$

In terms of these quantities, the power laws found by Carnevale *et al.* [7] for $r(t)$, $\rho(t)$, $a(t)$, and $Z(t)$ read:

$$r(t)\sim\lambda\left[\frac{t}{\tau}\right]^{\xi/2},\quad \rho(t)\sim\lambda^{-2}\left[\frac{t}{\tau}\right]^{-\xi},\quad a(t)\sim\lambda\left[\frac{t}{\tau}\right]^{\xi/4},\quad Z\sim\tau^{-2}\left[\frac{t}{\tau}\right]^{-\xi/2}, \tag{3}$$

where ξ is a free parameter. By setting $\xi=0.75$, the authors found good agreement with the numerical results of Ref. [4]. Laws consistent with (3) have been found in a discrete vortex system model [8]. Actually, the subject is far from being closed since other numerical studies do not reveal so explicitly the existence of power laws [9,10] or find different exponents [11].

On the experimental side, the decay of quasi-two-dimensional turbulence has been studied, some years ago, in rotating tanks and in stratified systems [12], and in horizontal soap films [13]. Such experiments revealed many interesting features of quasi-two-dimensional systems, such as merging, dipole propagation, and emergence of coherence structures; actually, due to the large experimental uncertainties on the measurement of the flow field, it has been difficult to extract accurate information on the decay laws themselves. More recently, two of the present authors [14] performed similar studies in a thin layer of electrolyte, finding results apparently consistent with the theory of Carnevale *et al.* [7]. All these studies actually suffer from the absence of reliable measurements of the local velocity, from which the vorticity field could be deduced. The aim of the present study is to achieve such measurements by using particle image velocimetry. From these measurements, we shall be in a position to characterize our system both geometrically and dynamically, and further proceed to a quantitative comparison with the existing theories. The result will be somewhat surprising, since unexpected characteristics for the turbulence will be found. We report here and discuss the corresponding results.

II. EXPERIMENTAL SETUP

A. Experiment

The experimental arrangement, which is shown in Fig. 1, is similar to the one used in a precedent study. The cell is machined out of PVC and the bottom of the cell is a thin layer (1-mm thick) of glass. Permanent magnets are located just below the bottom of the cell. They are samarium cobalt parallelepipeds, $5\times8\times3$ mm^3 in size and their magnetization axes are vertical. Each magnet produces a magnetic field which has a maximum value of 0.34 T and decay over a typical length of 3 mm. The magnets are put together to form a square array of alternated poles. It is possible to use an arbitrary number of magnets, up to 14×13. The flow itself is confined horizontally by solid rectangular rods. The cell is filled with a normal solution of sulfuric acid to match the height of the rods; by this way, we suppress any meniscus effect on the boundaries. An electric current I is driven through the electrolyte from one side of the cell to the other. It is supplied by a constant current source, regulated to 10^{-4}, and controlled by a computer. The fluid is thus subjected to an electromagnetic force, stationary in time and periodic in space. The period of the forcing is twice the length of a magnet, i.e., 16 mm, and its magnitude is controlled by I. For a current of 300 mA (which is a typical value), the Reynolds number calculated on the size of the cell is about 2000. The flow is visualized by using clusters of neutrally buoyant particles, several tens of micrometers in size. The particles are made visible by illuminating the fluid with an halogen lamp. The images of the flow are taken with a video camera located above the experimental cell, and recorded on a Umatic video take recorder.

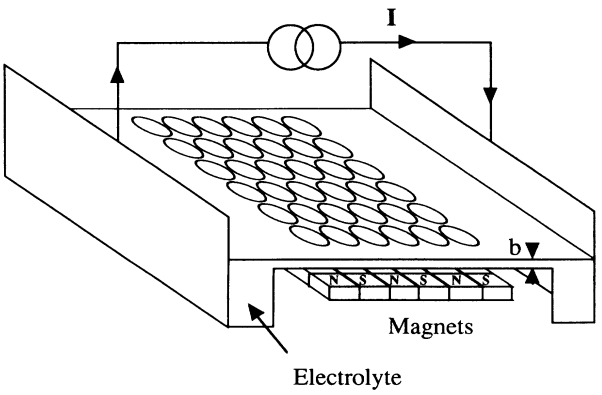

FIG. 1. Schematic representation of the experimental system (not to scale); the walls confining the flow and the lateral limits of the cell are not represented.

The experimental procedure consists in imposing an electric current I at time $t=-\tau$ switching it off at $t=0$, and leaving the system relaxing to an equilibrium state. During the process, an audio signal is generated by the computer and recorded on the sound channel of the video tape recorder, so as to identify each frame of the video signal. In a second step, the video frames are digitized, ordered, and stored on a magneto-optical disk.

B. Experimental determination of the velocity field

The calculations are performed on a Macintosh II fx computer, assisted by a double digital signal processor card DSP32C. The method which we use consists in discretizing the flow surface on a squared grid and computering, for each node, the correlation, on a square cell of size $(\lambda\times\lambda)$ centered around the node, of the intensity field between two images separated by a time interval δt. The position of the maximum of correlation provides the information on the local coarse-grained velocity, with a spatial resolution equal to the size of the cell itself. We usually discretize the flow domain into a 32×32 grid. The choice of the summary of the elementary cell λ is guided by the following considerations:

(1) It is much smaller than a typical scale of variation of the flow.

(2) It contains many particles, so as to take advantage of statistical averaging. In practice, a mean number of 5 particles per cell is a minimal value.

(3) Most of the particles stay within the cell during the interval of time δt. This introduces some limitations on the largest measurable velocity.

For the flows which we consider, a typical size which meets all these criteria is 32 pixels. The choice of δt also requires some adjustment: for a given cell size, it must satisfy condition (3), and be such that the displacement of the particles is measurable. In practice, we adjust δt for the mean displacement of the particles, which we measure to lie between 1.7 and 2.5 pixels.

Even when all the above criteria are met, we may obtain, in some cells, aberrant data. To check the validity of the measurement, we compute the local divergence of the velocity field and, if it exceeds some threshold value,

we replace the actual velocity by a local average of the neighboring values. The resulting velocity field is further interpolated on a 128×128 points lattice. Fourier transformed, and low-pass-filtered at half the Nyquist frequency (i.e., the fourth of the sampling frequency). The vorticity field and the stream function are computed in the spectral space, and backtransformed into the real space. A typical result of such a calculation is shown in Fig. 2. In this case, the flow was initially composed of 10 vortices, and Fig. 2 corresponds to a state obtained one second after the quench. Figure 2(a) represents the direct image of the flow averaged over 0.20 s. Figures 2(b), 2(c), and 2(d) represent, respectively, the velocity field, the stream function, and the vorticity field. It is instructive to compare the stream-line patterns of Figs. 2(a) and 2(c). The agreement between the two images is excellent and, in the mean, the differences between them can be estimate to a few percent. One can infer that the error on the vorticity field is typically lower than 20%. This estimate is in agreement with the amplitude of the fluctuations ob-

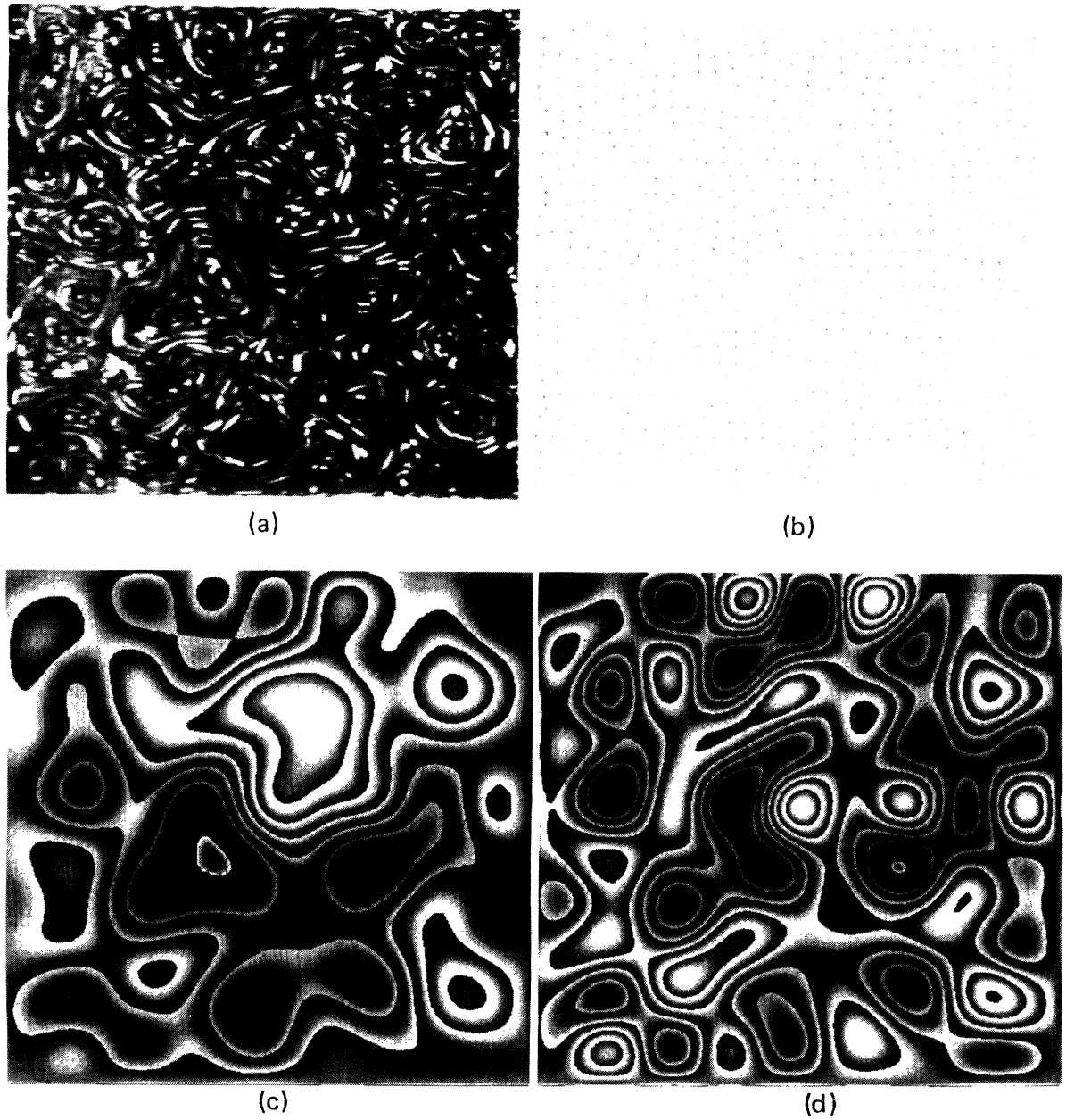

FIG. 2. Freely decaying turbulence from an ordered lattice of 100 vortices obtained at $I=300$ mA for 1.2 s, with a thickness $b=3$ mm. Image of the flow is taken 1 s after the sudden quench of the electric current. The size of the system (80×80 mm^2) gives the scale of the figures: (a) direct image of the flow average over 10 frames ($\frac{1}{5}$ s); (b) corresponding velocity field computed using correlation zone of size $\lambda=32$ and a time interval $\partial t=0.04$ s; (c) computed stream function based on the velocity field (b); (d) computed vorticity field based on the velocity field (b).

served from one image to the next one, in conditions where the time separation is so small that we expect a continuous evolution.

When the velocity field is determined, we calculate various global quantities characterizing the flow, such as the energy E and the enstrophy Z defined as

$$E=\int u^2 dS=\int E(k)dk$$

and

$$Z=\int \omega^2 dS=\int k^2 E(k)dk \ ,$$

where $E(k)$ is the Fourier component of the energy, at wave number $k=\sqrt{k_x^2+k_y^2}$, where k_x and k_y are the component, in the spectral plane, of wave vector $\mathbf{k}$. We also determine the geometrical properties of the flow, characterized by the number of vortices or the vortex density $\rho(t)$, their mean size at $a(t)$, and the mean separation distance $r(t)$ between vortices. There is no ambiguity in defining the vortex size by the relation

$$a(t)=\sqrt{E/Z} \ .$$

The other quantities are more delicate to define, and may involve some ambiguity. It turns out that in our system, the local maxima of the vorticity field tend to form clusters [see Fig. 2(d)]. The criterium that we use assimilate such clusters to vortices. In practice, we carry out the calculation on the stream function rather than the vorticity field, since vortex clusters turn out to correspond to well-defined extrema on this map. This can be checked easily for small clusters in Fig. 2(d). The procedure thus consists in determining the extrema of the stream function and counting and localizing them, so as to get the vortex density $\rho(t)$ and the mean separation $r(t)$.

Concerning the computational time, it takes about 1 min to compute the velocity field on a 32×32 grid. Since we calculate about 200 images in a typical experiment, the total computational time is therefore a few hours in this case.

III. RESULTS

A. Qualitative aspects

As explained above, the experimental procedure that we use consists in imposing an electric current I for a short period of time (a fraction of second) and then turning it off. Figures 3 and 2(d) represent the vorticity field for $t=0$ and $t=1$ s, respectively, for the case of an initially ordered pattern. We observe that the system undergoes a rapid sequence events leading to the formation of large structures. Perhaps the most important dynamical event is the merging of like-sign vortices. Figure 4 represents such a phenomenon, obtained in the decay regime of a system of 36 vortices. The first step corresponds to the appearance of a large-scale flow embedding the two like-sign vortices [see Fig. 4(b)]. In a second step, one eddy increases at the expense of the other, which further disappears; the final stage is the axisymmetrization of the resulting eddy [see Fig. 4(d)]. Such a sequence of

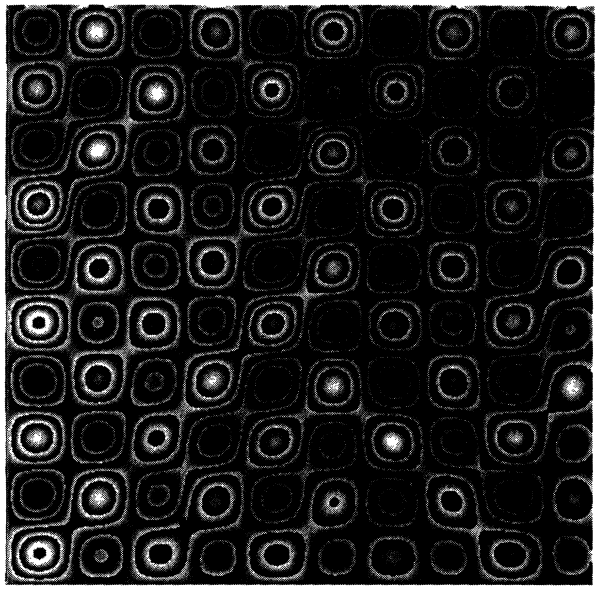

FIG. 3. Vorticity at $t=0$ for the same condition as in Fig. 2.

events takes a fraction of second to be completed; we may also have aggregation phenomena, for which traces of the initial structure of the eddies never completely disappeared and which are not limited to two vortices. Figures 2(a) and 2(c) show aggregation of like-sign vortices involving at least three vortices. This occurs mostly at late times in the decay process. Another interesting event is the formation of dipoles, as shown on Fig. 5. When a dipole nucleates, it propagates for a fraction of second, after which it breaks and merges with other structures of the lattice. This time thus seems to be a typical life duration for a dipole. Dipole formation is actually not frequent in our experiment and tripole formations have never been observed. Another qualitative aspect, already mentioned, is that the large-scale eddies usually correspond to clusters of vortices, rather than isolated vortices. The clusters themselves have a size comparable to their mean separation, so that our system resembles a dense assembly of clusters of vortices, rather than a population of well-separated vortices. This aspect will be made more precise below.

B. Quantitative results and scaling laws

Figure 6 represents the evolution of the total kinetic energy $E(t)$, and the enstrophy $Z(t)$ in cases where the lattice is initially ordered. These quantities increase up to $t=0$, and further decay. The decrease of the energy is exponential, with a time constant of about 2.3 s; this value is close to the viscous decay time $\tau_v=2b^2/3\nu$, which corresponds to the viscous damping against the bottom wall for the case of Poisseuilles-type flows. Then one observes that the energy is essentially burnt by laminar friction against the bottom wall. The enstrophy also decreases, but, in a first period, i.e., from 0 to about 3 s, faster than the energy. This period coincides with the oc-

currence of many merging events. Beyond this period, the flow pattern no longer evolves and we find that the two quantities decay at the same rate (see Fig. 6). We further focus on the first period, where the interesting phenomenology takes place.

Figures 7 and 8 summarize the results which we have obtained, restricted to the first three seconds of decay, for initially ordered conditions, several lattice sizes, various energy levels, and a fluid thickness $b=3$ mm. Beyond that time, no further evolution is observed. Figure 7 shows geometric quantities [the vortex size $a(t)$, the vortex density $\rho(t)$, the distance between eddies $r(t)$], while Fig. 8 represents dynamical quantities, such as the normalized enstrophy $Z(t)/E(t)$, the normalized maximum vorticity $\omega_{\text{ext}}/\sqrt{E}$, and the kurtosis of the vorticity distribution $K(t)$. (Note actually that ω_{ext} does not have the same meaning as in Ref. [7]. In our case, ω_{ext} is the extremum of the vorticity field, while in Ref. [7], ω_{ext} is the average vortex amplitude.) A remarkable result that we

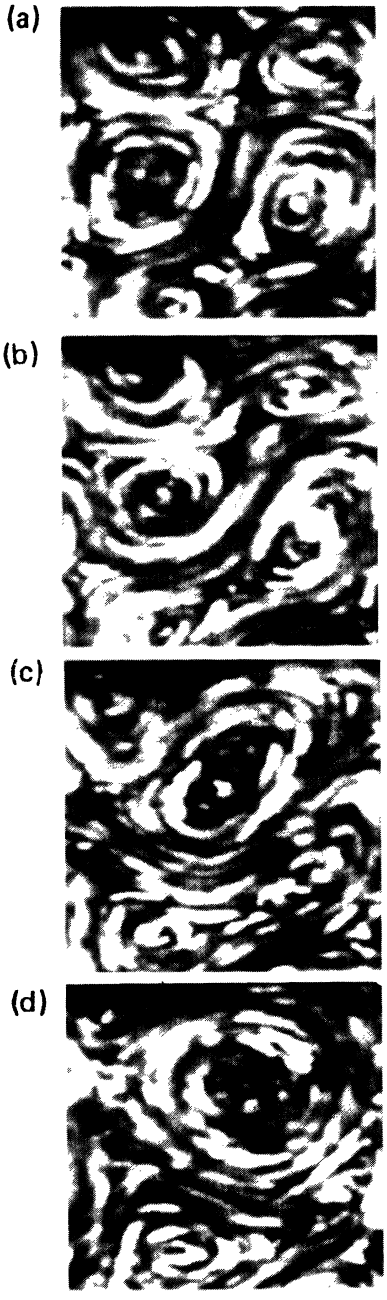

FIG. 4. Merging of two like-sign vortices. (a) initial state ($t=0$ s); (b) apparition of a large-scale flow embedding the two like-sign vortices ($t=0.14$ s); (c) the two vortices are attracted to each other, the smallest one decrease to the benefit of the largest one ($t=0.40$ s); (d) symmetrization of the final vortex ($t=0.70$ s).

FIG. 5. Dipole evolution. The time interval between two successive images is 0.05 s. The dipole is a stable structure that can survey in the flow for a very long period of time.

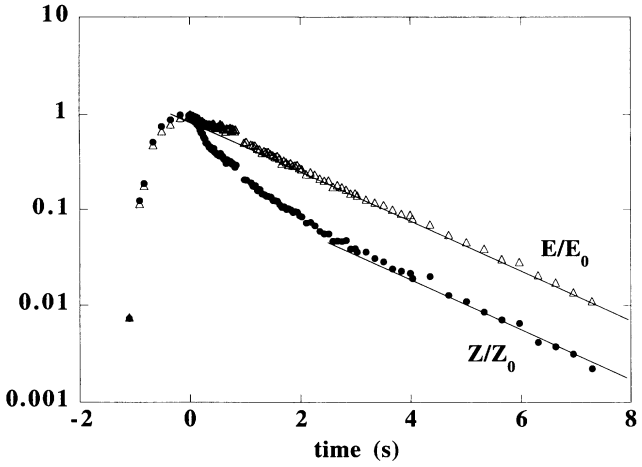

FIG. 6. Decay of the energy and the enstrophy for a system of 100 vortices, with $b=3$ mm, an initial value of I of 400 mA, and $\tau=100$ ms (the ordinates have been renormalized to 1 for $t=0$).

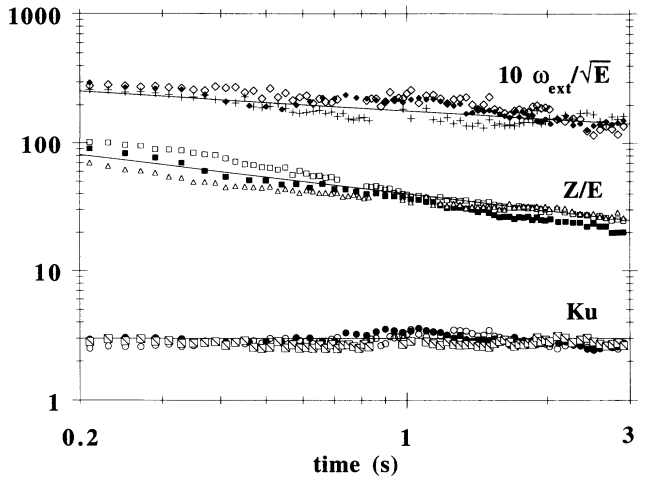

FIG. 8. Temporal evolution of the enstrophy Z (divided by E), the vorticity kurtosis Ku, and the extremum vorticity ω_{ext} (divided by $\sqrt{E}$), for conditions similar to those of Fig. 7.

obtain is the existence of power laws for all these quantities, throughout one decade of time variation. Power laws are best defined when the lattice is initially ordered, but they are also observed, with comparable exponents, for other experimental conditions, such as disordered initial state, system of tripoles, quadrupoles, various thicknesses (ranging between 2.5 and 4 mm), and various initial energies.

The uncertainty on the value of the exponents characterizing the power laws of Figs. 7 and 8 must be discussed. The main uncertainty on the exponents has a statistical origin: to show this, we have performed a series of seven experiments, with comparable initial conditions, the same number of vortices, and the same fluid-layer thickness; for a single run, we find an exponent comprised between -0.15 and -0.25, and a mean value of -0.22. The scatter is thus large, but the mean value seems reliable. With this restriction, we obtain the following values for the exponents of Figs. 7 and 8, together with rough estimate for the incertainties

$$\rho \approx t^{-0.44\pm0.1}, \quad r \approx a \approx t^{0.22\pm0.03},$$

$$\frac{\omega_{ext}}{\sqrt{E}} \approx t^{-0.22\pm0.06}, \quad \frac{Z}{E} \approx t^{-0.44\pm0.06}.$$

Another, simpler description of our system can be done by noting that system remains dense during the decay phase. This is shown in Fig. 9, which represents the evolution of ρa^2 (which is a measure of the space occupied

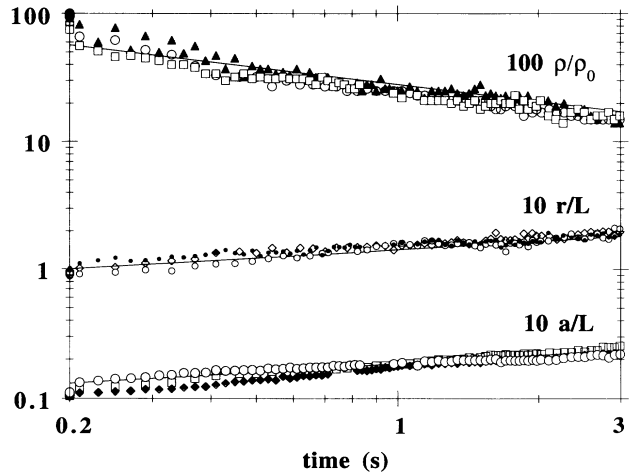

FIG. 7. Temporal evolution of the vortex densities ρ/ρ_0 (where ρ_0 is the value for $t=0$), the mean distance between vortices $r(t)/L$, and the mean vortex sizes $a(t)/L$ (where L is the system size), for systems of 100 vortices, $b=3$ mm, and several initial values of the energy, corresponding to values of the Reynolds number $\sqrt{E}L/\nu$ of the order of 1000.

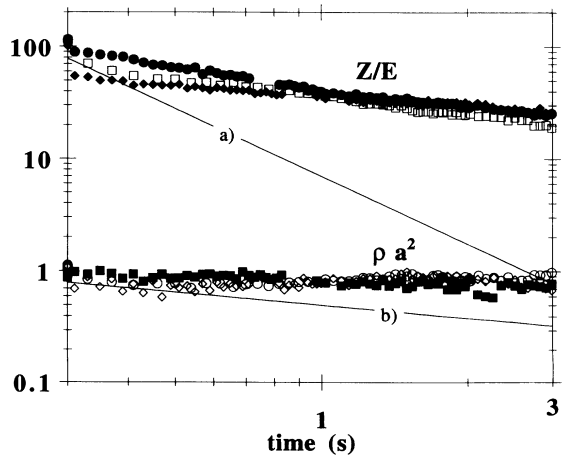

FIG. 9. (a) Experimental plot for Z/E and comparison with Batchelor theory [6]. (b) Experimental plot for ρa^2 and comparison with theory of Carnevale *et al.* [7]. The experimental conditions are similar to those of Fig. 7.

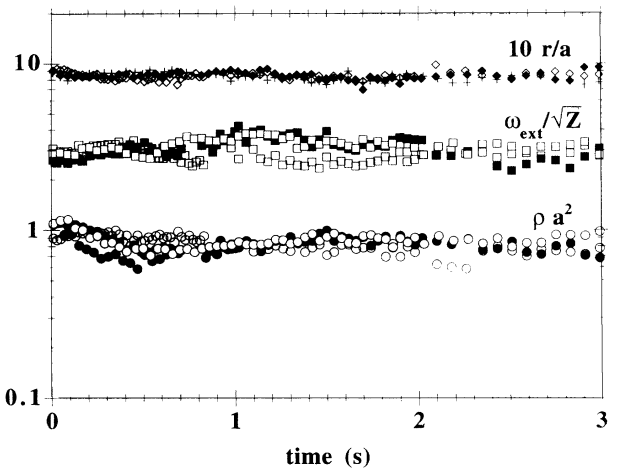

FIG. 10. Several quantities which appear as invariant in the system: ρa^2, $\omega_{ext}/\sqrt{Z}$, and r/a; the experimental conditions are similar to those of Fig. 7.

by the vortices), and that of the ratio r/a. Both quantities are conserved during the decay phase. The fact that the value of r/a is about 1 indicates that the system is dense. Another indicator revealing the same feature is the kurtosis, which is found constant during the decay phase. It thus appears that the vortices occupy almost all the available space and there is no rarefaction process. If the vortices were assimilated to molecules, our system would resemble a liquid.

The dynamical signature of this characteristics seems to be the fact that the maximum vorticity decreases as rapidly as the square root of the enstrophy (see Fig. 10). One can show, by using order of magnitude arguments, similar to those of Ref. [7], that the same scaling law applies to the two quantities when the vortices occupy all the available space. All the scaling which we find thus seems consistent. To describe our turbulent flow, we propose the following laws:

$$a(t)\sim r(t)\sim\sqrt{1/\rho(t)}\sim t^{\nu},$$

$$Z\sim\omega_{ext}^2\sim Et^{-2\nu},\quad K\sim\text{const},$$

with $\nu=0.22\pm0.04$. This estimate for ν includes all the experiments which we have performed, with ordered and disordered initial conditions, depths varying between 2.5 and 4 mm and various energy levels.

IV. DISCUSSION AND CONCLUSION

We now compare our results to the theoretical predictions discussed in the Introduction. If we consider first the Batchelor theory, we find qualitative agreement, concerning the fact that the system remains filled with the vortices during the decay phase. However, we do not observe the predicted exponents and the discrepancies on the corresponding values are important. Figure 9 shows an example of the difference found between this theory and our results, for the ratio of the enstrophy over the energy. Theory predicts t^{-2} whereas we find $t^{-0.44}$.

If we now consider the theory of Carnevale *et al.* [7], we find that some experimental values of the exponents are not far from the predictions. This is the case for all mean vortex size, which increases like $t^{0.22}$ in the experiment, while the prediction is $t^{0.18}$. Actually, the exponents for the vortex density are different, and large deviations are observed when we compare the evolution of the kurtosis. Also, in our experiment, the maximum vorticity decreases as the square root of the enstrophy; it is thus difficult to consider ω_{ext} as an invariant. There are in fact qualitative differences between this theory and our experiment: the theory predicts that, during the decay process, the surface occupied by the vortices decreases, and rapidly, the flow becomes a dilute system of vortices. In our case, such an evolution is not observed: it remains densely filled with vortex clusters. This difference is evident when we compare Fig. 1 of McWilliams [4] with our Fig. 2(b). Our values of ρa^2 and r/a (which are the space occupied by the vortices and the average distance between eddies) are of order 1, whereas those typically used in numerical experiment are several order of magnitude smaller (see, for instance, Refs. [3] and [4]).

To explain the differences between our results and the previous numerical studies, several possibilities exist: indeed our experiment is not a purely two-dimensional system, since, like any other experiment, it lives in a three-dimensional world. This can be an origin of the discrepancies between our results and the numerical studies, although it is difficult to know more precisely where three-dimensionality comes in. Another difference which can be outlined is that in our system the dissipation rate is much larger than in the numerical models. We believe that this has no significant consequence, since the exponents which we measure are determined in the first second of the decay phase, and in this period, the energy has decreased by less than 30%. It would be interesting indeed to be in position to work with a smaller dissipation; an experiment using mercury is now in preparation. In the same spirit, one could argue that our regime of decay corresponds to a first period and if the dissipation was small enough, we would recover the numerical observations. It would thus be interesting to investigate numerically if, eventually, liquid turbulence is observed at early times. This is probably an interesting issue, because there are not so many opportunities in the field of two-dimensional turbulence where a link between the numeric and the real world can be established.

ACKNOWLEDGMENTS

We are grateful to M. E. Brachet, B. Legras, Y. Pomeau, and H. Willaime for interesting discussions. This work has been supported by Centre National de la Recherche Scientifique, Nicole Normale Supérieure, Universités Paris 6 and Paris 7.

[1] J. C. McWilliams, J. Fluid Mech. **146**, 21 (1984).
[2] M. E. Brachet, M. Meneguzzi, H. Politano, and P. L. Sulem, J. Fluid Mech. **194**, 333 (1988).
[3] R. Benzi, S. Patarnello, and P. Santangelo, J. Phys. A **21**, 1221 (1988).
[4] J. C. McWilliams, J. Fluid Mech. **219**, 361 (1990).
[5] B. Legras and D. Dritschel (unpublished).
[6] G. K. Batchelor, Phys. Fluids Suppl. II **12**, 233 (1969).
[7] G. F. Carnevale, J. C. McWilliams, Y. Pomeau, J. B. Weiss, and W. R. Young, Phys. Rev. Lett. **66**, 2735 (1991).
[8] G. Huber and P. Alstrom, Physica A **195**, 448 (1993).
[9] W. H. Matthaeus, W. T. Stirbling, D. Martinez, S. Oughon, and D. Montgomery, Physica D **51**, 531 (1991).
[10] W. H. Matthaeus, W. T. Stirbling, D. Martinez, S. Oughon, and D. Montgomery, Phys. Rev. Lett. **66**, 2731 (1991).
[11] D. G. Dritschel, Phys. Fluids A **5**, 984 (1993).
[12] E. Hopfinger, R. W. Griffiths, and M. Mory, J. Mec. Theor. Appl. **2**, 21 (1983).
[13] Y. Couder, C. R. Acad. Sci. **297**, 641 (1983).
[14] P. Tabeling, S. Burkhart, O. Cardoso, and H. Willaime, Phys. Rev. Lett. **67**, 3772 (1991).

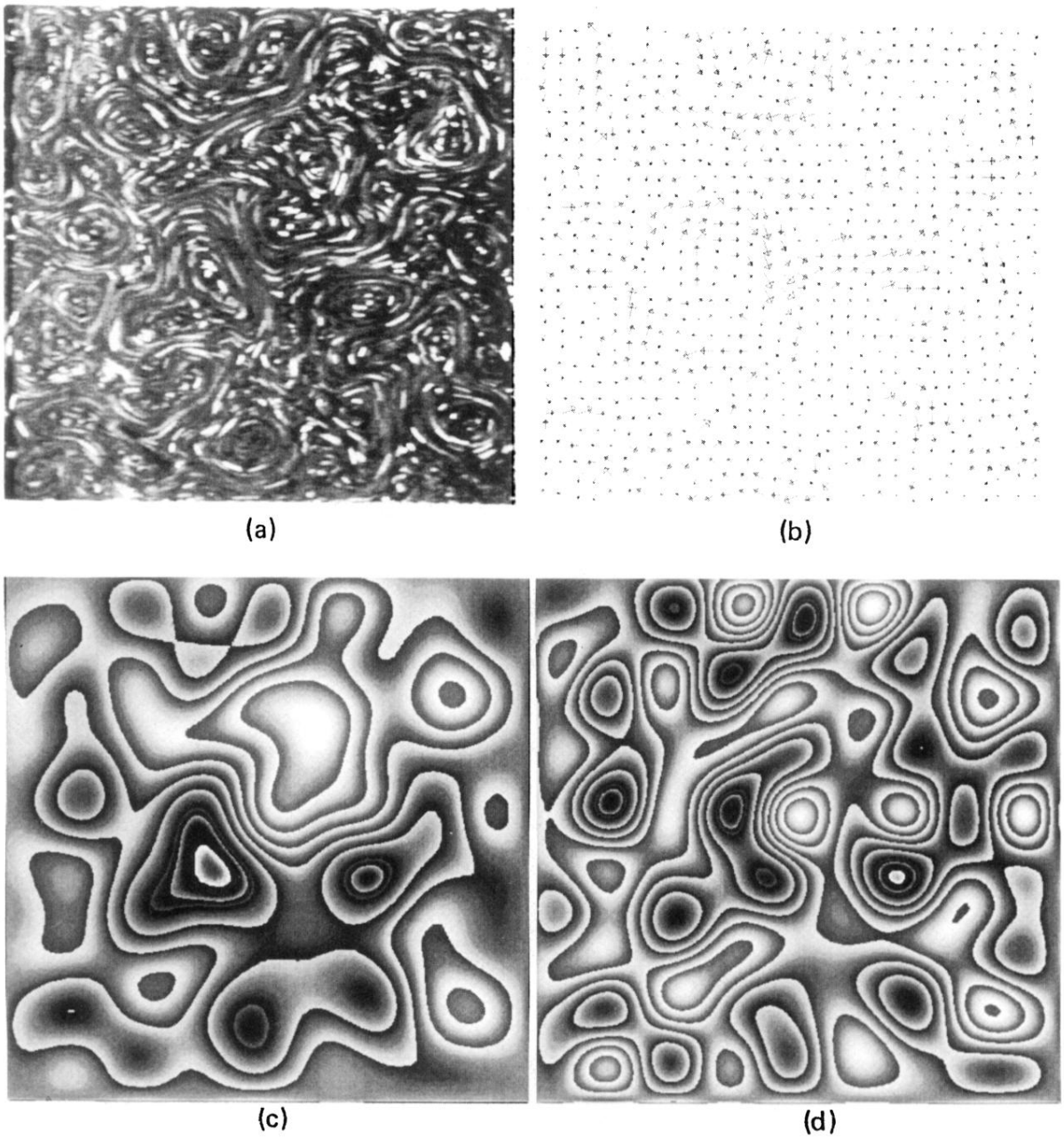

FIG. 2. Freely decaying turbulence from an ordered lattice of 100 vortices obtained at $I = 300$ mA for 1.2 s, with a thickness $b = 3$ mm. Image of the flow is taken 1 s after the sudden quench of the electric current. The size of the system (80×80 mm^2) gives the scale of the figures: (a) direct image of the flow average over 10 frames ($\frac{1}{5}$ s); (b) corresponding velocity field computed using correlation zone of size $\lambda = 32$ and a time interval $\partial t = 0.04$ s; (c) computed stream function based on the velocity field (b); (d) computed vorticity field based on the velocity field (b).

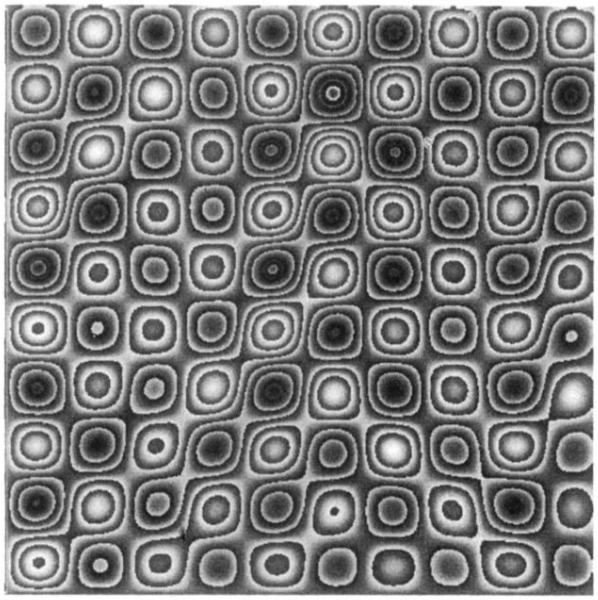

FIG. 3. Vorticity at $t = 0$ for the same condition as in Fig. 2.

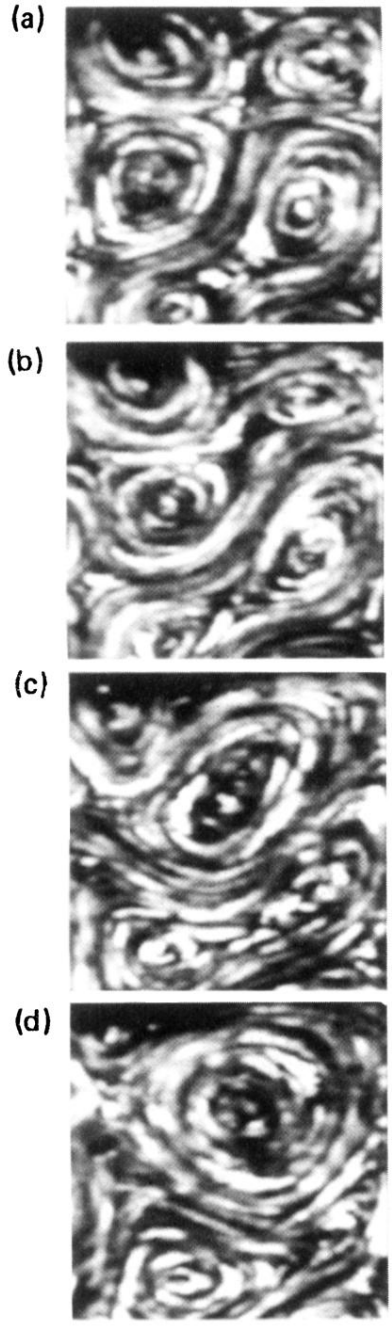

FIG. 4. Merging of two like-sign vortices. (a) initial state ($t=0$ s); (b) apparition of a large-scale flow embedding the two like-sign vortices ($t=0.14$ s); (c) the two vortices are attracted to each other, the smallest one decrease to the benefit of the largest one ($t=0.40$ s); (d) symmetrization of the final vortex ($t=0.70$ s).

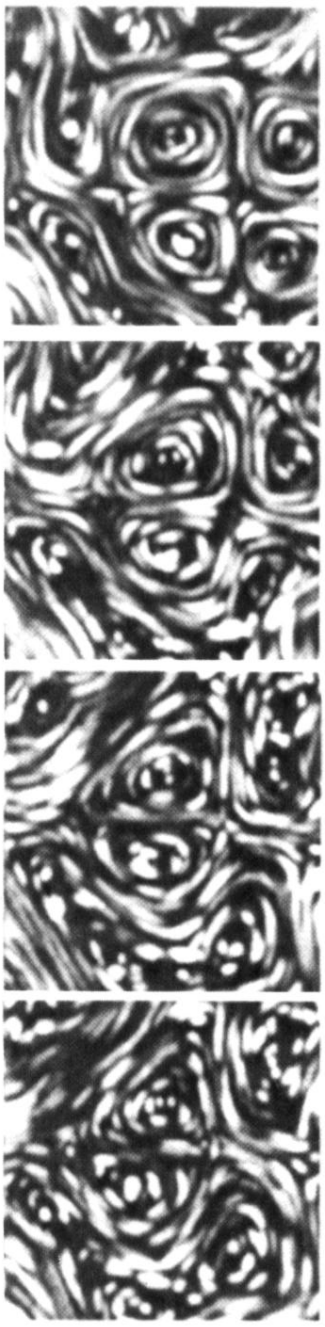

FIG. 5. Dipole evolution. The time interval between two successive images is 0.05 s. The dipole is a stable structure that can survey in the flow for a very long period of time.